

We are IntechOpen, the world's leading publisher of Open Access books Built by scientists, for scientists

6,900

Open access books available

186,000

International authors and editors

200M

Downloads

Our authors are among the

154

Countries delivered to

TOP 1%

most cited scientists

12.2%

Contributors from top 500 universities



WEB OF SCIENCE™

Selection of our books indexed in the Book Citation Index
in Web of Science™ Core Collection (BKCI)

Interested in publishing with us?
Contact book.department@intechopen.com

Numbers displayed above are based on latest data collected.
For more information visit www.intechopen.com



Modeling the Magnetocaloric Effect of $\text{Nd}_{0.67}\text{Ba}_{0.33}\text{Mn}_{0.98}\text{Fe}_{0.02}\text{O}_3$ by the Mean Field Theory

Mohamed Hsini and Sadok Zemni

Abstract

In this paper, we have exploited the mean field theory combined with the Bean-Rodbell model to justify the magnetocaloric effect (MCE) in $\text{Nd}_{0.67}\text{Ba}_{0.33}\text{Mn}_{0.98}\text{Fe}_{0.02}\text{O}_3$ sample. The simulation of some magnetic properties has been investigated. Modeling magnetization curves have been successfully achieved using this model. The second-order ferromagnetic-paramagnetic (FM-PM) phase transition of our system has been verified through the value of the parameter which controls the transition nature in the Bean-Rodbell model. Theoretical and experimental expressions, which have rated the magnetic entropy change ($-\Delta S_M$) under various magnetic fields, have been derived. Theoretical ($-\Delta S_M$) curves have been compared to the experimental ones.

Keywords: mean field theory, Bean-Rodbell, magnetocaloric effect, magnetization, magnetic entropy change

1. Introduction

In recent years, magnetic materials exhibiting high magnetocaloric effect (MCE) have been extensively studied experimentally and theoretically because of their intensive necessity in magnetic refrigeration (MR) [1–3]. This recent cooling technology, which is expected to replace traditional expansion/compression gas refrigeration technology, has many particular interests because of its significant economic benefits [4–6]. The magnetic entropy change ($-\Delta S_M$) is interestingly important for rating the refrigerant properties [7, 8]. Thus, numerous materials exhibiting high MCE have been widely developed in the last decades for exploitation as promising materials in MR technology [9–14].

The mean field model [15, 16] is an efficient tool in the study of magnetic materials [17]. Currently, Amaral et al. have signaled a scaling method based on this model [18].

According to the work of Amaral et al., we have reported, in this paper, our studies on the magnetocaloric properties of the $\text{Nd}_{0.67}\text{Ba}_{0.33}\text{Mn}_{0.98}\text{Fe}_{0.02}\text{O}_3$ sample which exhibits a second-order ferromagnetic-paramagnetic (FM-PM) phase transition [19], by scaling the experimental magnetization. We have showed, in this work, how the mean field theory may adequately model the magnetic and the magnetocaloric properties of this magnetic system, which may be applicant in MR technology.

The scaling method based on the mean field model leads us to estimate directly the saturation magnetization (M_0), the exchange parameter (λ), the total angular momentum (J), and the Lande factor (g) of our sample. These parameters are necessary for simulating magnetization isotherms, $M(H, T)$, which are used for the calculation of the magnetic entropy change ($-\Delta S_M$) of $\text{Nd}_{0.67}\text{Ba}_{0.33}\text{Mn}_{0.98}\text{Fe}_{0.02}\text{O}_3$ material. In addition, the second-order phase transition FM-PM of this sample is confirmed by analyzing the Bean-Rodbell model [20, 21].

2. Theoretical and experimental study

2.1 Brief overview of the experimental study

In this section, we have summarized the primary results of the structural and magnetic analysis of the manganite sample $\text{Nd}_{0.67}\text{Ba}_{0.33}\text{Mn}_{0.98}\text{Fe}_{0.02}\text{O}_3$ reported in our precedent work [19].

This compound has been prepared by the solid-state ceramic method at 1400°C in a polycrystalline powder form. Rietveld structural analysis has showed a good crystallization of the sample which presents a pseudo-cubic structure of orthorhombic Imma distortion, with unit cell parameters $a = 0.54917$ (1), $b = 0.77602$ (1), $c = 0.551955$ (4) nm, and unit cell volume $V = 0.235228$ (3) nm^3 . Scanning electron microscope (SEM) analysis has indicated that the sample presented a homogeneous morphology which consists of well-formed crystal grains. The SEM analysis coupled with the EDX has confirmed that the chemical composition of the sample is close to that nominal reported by the above chemical formula (19).

The evolution of the magnetization as a function of temperature, under a 0.05 T magnetic applied field in FC and ZFC modes, is depicted in **Figure 1**. This figure shows a FM-PM transition at a Curie temperature which has been estimated in the inset by determining the minimum value of the derivative magnetization versus temperature in ZFC mode at 0.05 T applied field ($T_C = 131$ K). However, **Figure 1** shows a non-negligible monotonic decrease of the magnetization between 10 and 100 K. This indicates a canted spin state between the Nd^{3+} and the (Mn^{3+} , Mn^{4+}) spin sub-lattices, with canted angle, θ , assumed to be between 0° (ferromagnetic coupling) and 180° (antiferromagnetic coupling).

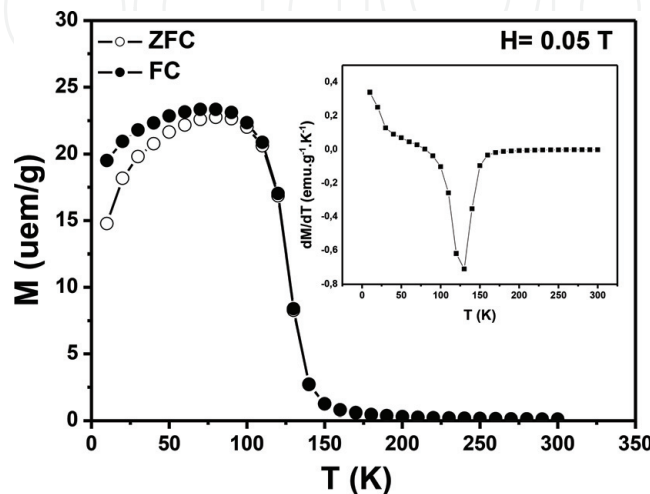


Figure 1.

M versus T in 0.05 T applied magnetic field for the $\text{Nd}_{0.67}\text{Ba}_{0.33}\text{Mn}_{0.98}\text{Fe}_{0.02}\text{O}_3$ versus T in FC and ZFC modes. The inset is $\frac{dM}{dT}$ versus T for ZFC mode.

Figure 2 shows the variation of the magnetization as a function of the varied magnetic field up to 10 T, at very low temperature (10 K), for the undoped compound $Nd_{0.67}Ba_{0.33}MnO_3$ and for the doped compound $Nd_{0.67}Ba_{0.33}Mn_{0.98}Fe_{0.02}O_3$.

It is apparent in this figure that in spite of the intense magnetic applied field (10 T), the magnetization does not attain saturation. This is due to the presence of the magnetic moments of Nd^{3+} ($[Xe] 4f^3$) which have three electrons in the 4f orbital. Effectively, a comparison between magnetization of the two compounds $Nd_{0.67}Ba_{0.33}MnO_3$ [19] and $La_{0.67}Ba_{0.33}MnO_3$ [22] are depicted in **Figure 3**. This figure shows obviously that the lanthanum compound rapidly reaches saturation even under low applied magnetic field. This is because of the non-contribution of the La^{3+} ion ($[Xe]$) in magnetism which has no electrons in 4f orbital. **Figure 2** also indicates that a 2% iron doping proportion in $Nd_{0.67}Ba_{0.33}Mn_{0.98}Fe_{0.02}O_3$ decreases the magnetization by $0.12\mu_B$ ($3.94\mu_B$ for $Nd_{0.67}Ba_{0.33}MnO_3$, whereas $Nd_{0.67}Ba_{0.33}Mn_{0.98}Fe_{0.02}O_3$ presents $3.82\mu_B$) under a 10 T applied magnetic field of, in a good agreement with an antiferromagnetic coupling between Mn^{3+} and Fe^{3+} spin sub-lattices as demonstrated by the Mössbauer spectroscopy studies [23, 24]. As knowing, the orbital momentum is quenched by the crystal field in the octahedral site of manganite for transition elements, so only the spin of Fe^{3+} ($[Ar]3d^5$) contributes to

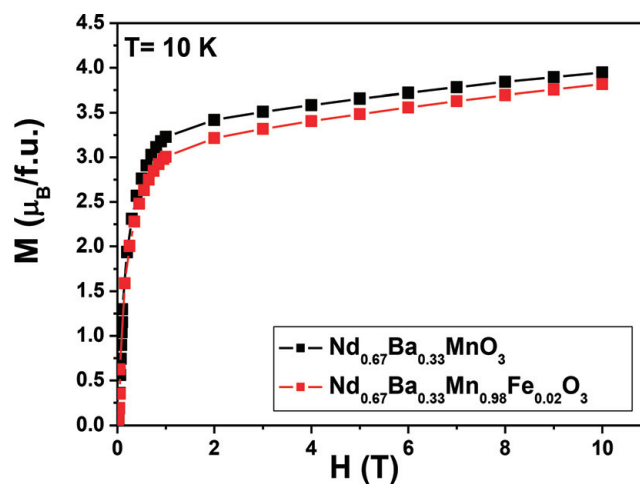


Figure 2.
 Comparison of M versus H at $T = 10$ K for $Nd_{0.67}Ba_{0.33}MnO_3$ and $Nd_{0.67}Ba_{0.33}Mn_{0.98}Fe_{0.02}O_3$ samples.

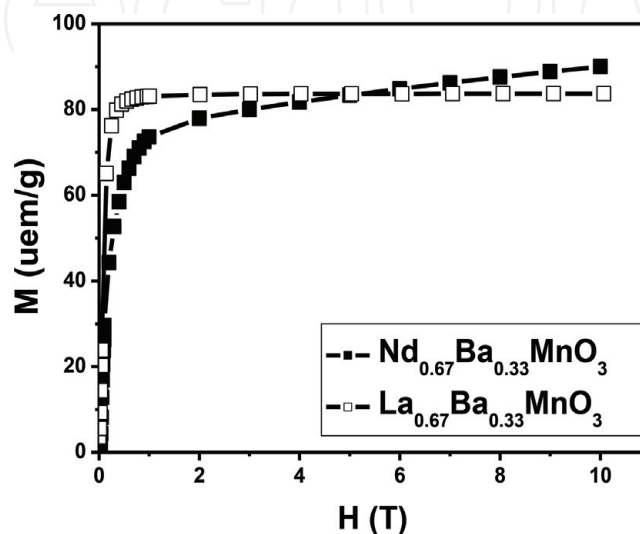


Figure 3.
 Comparison of M versus H at $T = 10$ K $La_{0.67}Ba_{0.33}MnO_3$ and $Nd_{0.67}Ba_{0.33}MnO_3$ for samples.

the magnetization; therefore, we have found that the experimental value ($0.12\mu_B$) is very near to that calculated ($M_{Fe^{3+}} = gS\mu_B = 0.02 \times 2 \times 5/2 \mu_B = 0.1\mu_B$).

2.2 Theoretical calculation

The magnetic moments of a ferromagnetic material, made under external magnetic field (H), tend to align in the H direction. The increase of parallel magnetic moments then leads to rising magnetization. Magnetization values could be rated by the Weiss mean field theory [15, 16, 18].

In fact, Weiss has enunciated that in a ferromagnetic, an exchange interaction between magnetic moments could be created, at least in a magnetic domain, where the magnetic moments could be ordered in a same direction. This interaction may be considered as an average over all interactions between a given magnetic moment and the other N magnetic moments of the Weiss domain. This internal interaction contributes to an exchange field or a Weiss mean field:

$$\vec{H}_W = \vec{H}_{exch} = \lambda \vec{M} \quad (1)$$

where λ is the exchange parameter and M is the magnetization of the ferromagnet, given by

$$M = M_0 B_J(x) \quad (2)$$

where

$$M_0 = NJg\mu_B \quad (3)$$

is the saturation magnetization,

$$B_J(x) = \frac{2J+1}{2J} \coth\left(\frac{2J+1}{2J}x\right) - \frac{1}{2J} \coth\left(\frac{x}{2J}\right) \quad (4)$$

is the Brillouin function, and

$$x = \frac{Jg\mu_B}{k_B} \left(\frac{H + H_{exch}}{T} \right) \quad (5)$$

where k_B is the Boltzmann constant, μ_B is the Bohr magnetron, N is the number of spins, and T is the temperature.

Eq. (2) can be written as a function of $\left(\frac{H+H_{exch}}{T}\right)$ as follows:

$$M(H, T) = f\left(\frac{H + H_{exch}}{T}\right) = M_0 \left[\frac{2J+1}{2J} \coth\left(\frac{2J+1}{2J} \frac{Jg\mu_B}{k_B} \left(\frac{H + H_{exch}}{T}\right)\right) - \frac{1}{2J} \coth\left(\frac{1}{2J} \frac{Jg\mu_B}{k_B} \left(\frac{H + H_{exch}}{T}\right)\right) \right] \quad (6)$$

Applying the reciprocal function f^{-1} of f , we can obtain the relations:

$$\frac{H}{T} = f^{-1}(M) - \frac{H_{exch}}{T}; H = Tf^{-1}(M) - \lambda M. \quad (7)$$

The magnetic entropy change can be expressed by the Maxwell relations [6, 25]:

$$\left(\frac{\partial S}{\partial H}\right)_T = \left(\frac{\partial M}{\partial T}\right)_H \quad (8a)$$

$$\left(\frac{\partial S}{\partial M}\right)_T = -\left(\frac{\partial H}{\partial T}\right)_M \quad (8b)$$

Using experimental isotherm magnetization data, measured at discrete values of both applied magnetic field and temperatures, and Eq. (8a), the magnetic entropy change can be approximated as

$$\Delta S_M(T, \Delta H) = \int_{H_1}^{H_2} \left(\frac{\partial M}{\partial T}\right)_H dH \approx \sum_n \frac{(M_{n+1} - M_n)_H}{T_{n+1} - T_n} \Delta H_n \quad (9a)$$

Eqs. (7) and (8b) allow us to determine the theoretical estimation of the magnetic entropy change:

$$\Delta S_M(T)_{H_1 \rightarrow H_2} = - \int_{M|_{H_1}}^{M|_{H_2}} \left(f^{-1}(M) - \left(\frac{\partial H_{\text{exch}}}{\partial T}\right)_M \right) dM \quad (9b)$$

To study the nature of the magnetic transition, we have called the Bean-Rodbell model to our magnetization data. As reported earlier [26–28], system exhibiting first- or second-order phase transitions have been interpreted using this model [29]. It considers that exchange interactions adequately depend on the interatomic distances; the Curie temperature T_C is expressed as follows:

$$T_C = T_0(1 + \beta\omega) \quad (10)$$

where $\omega = \frac{v-v_0}{v_0}$, v is the volume, v_0 presents the volume with no exchange interaction, and T_0 is the transition temperature if magnetic interactions are taking into account with no magneto-volume effects. β is the slope of the critical temperature curve on volume. The Gibbs free energy, for a ferromagnetic system, is given in Ref. [30] with the compressibility K , the magnetic entropy S , and the reduced magnetization $\sigma(\mathbf{x}) = B_J(\mathbf{x})$ as

$$G = -\frac{3}{2} \left(\frac{J}{J+1}\right) Nk_B T_C \sigma^2 - HgJ\mu_B N\sigma + \frac{1}{2K} \omega^2 - TS \quad (11)$$

The above free energy minimizes ($\frac{dG}{d\omega} = 0$) at

$$\omega = \frac{3}{2} \left(\frac{J}{J+1}\right) Nk_B K T_C \sigma^2 \quad (12)$$

Substituting Eq. (12) into Eq. (11) and minimizing G with respect to σ , according to the work of Zach et al. [29] and Tishin and Spichkin [6], we can obtain the magnetic state equation:

$$\sigma(Y) = B_J(Y) \quad (13)$$

with

$$Y = \frac{1}{T} \left[3T_0 \left(\frac{J}{J+1}\right) \sigma + \frac{gJ\mu_B}{k_B} H + \frac{9(2J+1)^4 - 1}{5 [2(J+1)]^4} T_0 \eta \sigma^3 \right] \quad (14)$$

where the parameter η checks the order of the magnetic phase transitions. For $\eta > 1$, the transition is assumed to be first order. For $\eta < 1$, the second-order magnetic phase transition takes place.

After combining Eq. (2) and Eq. (13), we have got two interesting equations, $M(x) = M_0 B_J(x)$ (giving simulated M versus H) and $M(Y) = M_0 B_J(Y)$ (giving simulated M versus T).

On the other hand, for weak values of x , the magnetization may be written as

$$M = M_0 g \mu_B \frac{H}{kT} \frac{J+1}{3} + \lambda M_0 g \mu_B \frac{1}{kT} \frac{J+1}{3} M = \chi H \quad (15)$$

The resolution of Eq. (15) gives easily the Curie-Weiss magnetic susceptibility:

$$\chi = \frac{NJ(J+1)g^2 \frac{\mu_B^2}{3k_B}}{T - \lambda NJ(J+1)g^2 \frac{\mu_B^2}{3k_B}} = \frac{C}{T - T_c} \quad (16)$$

where $T_c = \lambda C$ is the Curie temperature and C is the Weiss constant.

To determine accurately the exchange constant, we use the famous law of interaction between two magnetic atoms with spins \vec{S}_1 et \vec{S}_2 by the Hamiltonian [12]:

$$H = -2J\vec{S}_1\vec{S}_2 \quad (17)$$

given by Heisenberg, where J is the exchange constant.

If we consider an individual atom i with its magnetic moment $\vec{\mu}_i$ in a ferromagnetic system. This moment interacts with the external applied magnetic field \vec{H} and with the exchange field \vec{H}_{exch} . The total interaction energy is given as

$$E_i = -\vec{\mu}_i \left(\vec{H} + \vec{H}_{\text{exch}} \right) \quad (18)$$

From the Heisenberg model's viewpoint, the energy E_i of a ferromagnetic system is the sum of interaction energy of a given moment, $\vec{\mu}$, with the external field and that with all near neighbors to atom i . Let us consider that each atom has z near neighbors which can interact with spin i with the same force, i.e., that exchange parameter has the same value for all z neighbors. Then, the energy E_i may be written as

$$E_i = -\vec{\mu}_i \vec{H} - \sum_{k=1}^z 2J\vec{S}_i\vec{S}_k \quad (19)$$

where the index k runs over all z neighbors of the atom i .

It is practical to express the Heisenberg energy in Eq. 17 in terms of the atomic moments $\vec{\mu}$ rather than in terms of spins \vec{S} . It can be easily done if we consider that the relation between the spin and the atomic magnetic moment is $\vec{\mu} = -g\mu_B \vec{S}$. So, Eq. (19) would be rewritten as

$$E_i = -\vec{\mu}_i \left(\vec{H} + \frac{2J}{(g\mu_B)^2} \sum_{k=1}^z \vec{\mu}_k \right) \quad (20)$$

In fact, the two expressions of the energy E_i , in Eq. (18) and Eq. (20), are not similar. However, the sum term in Eq. (20) is not the same as \vec{H}_{exch} because it is the

interaction made by the individual spin i . But, \vec{H}_{exch} in the spirit of the Weiss theory presents the average of all interaction terms in the total system. As a result, we should carry out such averaging over all N atoms:

$$\vec{H}_{\text{exch}} = \left\langle \frac{2J}{(g\mu_B)^2} \sum_{k=1}^z \vec{\mu}_k \right\rangle = \frac{2J}{(g\mu_B)^2} \frac{1}{N} \left\langle \sum_i^N \sum_{k=1}^z \vec{\mu}_{i,k} \right\rangle \quad (21)$$

By summing on k , we could obtain

$$\vec{H}_{\text{exch}} = \frac{2J}{(g\mu_B)^2} \frac{1}{N} z \left\langle \sum_i^N \vec{\mu}_i \right\rangle = \frac{2J}{(g\mu_B)^2} \frac{1}{N} z \vec{M},$$

(then,)

$$E_i = -\vec{\mu}_i \left(\vec{H} + \frac{2Jz}{(g\mu_B)^2 N} \vec{M} \right) \quad (22)$$

Eq. (21) contains a term proportional to the magnetization, in perfect agreement with Weiss' postulate. We can write now

$$\vec{H}_{\text{exch}} = \frac{2Jz}{(g\mu_B)^2 N} \vec{M} \quad (23)$$

from which we immediately obtain the formula for Weiss' "effective field constant":

$$\lambda = \frac{2Jz}{(g\mu_B)^2 N} \quad (24)$$

Comparing this equation with Eq. (16), i.e., the phenomenological expression for λ , we obtain the solution for the critical temperature:

$$T_c = \lambda C = \frac{2Jz}{(g\mu_B)^2 N} \frac{NJ(J+1)g^2\mu_B^2}{3k_B} \quad (25)$$

Therefore

$$J = \frac{3k_B T_c}{2zJ(J+1)} \quad (26)$$

2.3 Mean field theory application

We begin by the determination of J , g , λ , and M_0 parameters, which are crucial for magnetocaloric effect simulation of $\text{Nd}_{0.67}\text{Ba}_{0.33}\text{Mn}_{0.98}\text{Fe}_{0.02}\text{O}_3$.

- Total angular momentum (J) determination

To determine the total angular momentum (J), we must quantify the canted spin angle, θ , between Nd^{3+} and (Mn^{3+} , Mn^{4+}) spin sub-arrays, using the difference between magnetizations of $\text{Nd}_{0.67}\text{Ba}_{0.33}\text{MnO}_3$ [19] and $\text{La}_{0.67}\text{Ba}_{0.33}\text{MnO}_3$ [22] samples at 10 T ($0.33\mu_B$) as shown in **Figure 3**. By writing the contribution of Nd^{3+} magnetic moment network (spin-orbit coupling) under the form

$M_{\text{Nd}^{3+}} = 0,67 J_{\text{Nd}^{3+}} g_{\text{Nd}^{3+}} \mu_B \cos \theta = 0,33 \mu_B$, where $J_{\text{Nd}^{3+}} = 4,5$ and $g_{\text{Nd}^{3+}} = 0,727$ are, respectively, the values of angular momentum and gyromagnetic factor for free ion Nd^{3+} as indicated in Ref. [16]. Therefore, we deduce.

$$\cos \theta = \frac{0,33}{0,67 J(\text{Nd}^{3+}) g(\text{Nd}^{3+})} = \frac{0,33}{0,67 \times 4,5 \times 0,727} = 0,15, \text{ so, } \theta = 81,34^\circ.$$

Using the Hund's rule for 4f orbital less than half full and the values of L and S indicated in Ref. [16] for Nd^{3+} , we obtain the value of the angular momentum of Nd^{3+} ion incorporated in $\text{Nd}_{0,67}\text{Ba}_{0,33}\text{Mn}_{0,98}\text{Fe}_{0,02}\text{O}_3$ sample:

$$J(\text{Nd}^{3+}) = 0,67 \times |L - S \times \cos \theta| = 0,67 \times \left| 6 - \frac{3}{2} \times 0,15 \right| = 3,869$$

As a result, the total angular momentum for $\text{Nd}_{0,67}\text{Ba}_{0,33}\text{Mn}_{0,98}\text{Fe}_{0,02}\text{O}_3$ sample is

$$\begin{aligned} J &= J(\text{Nd}^{3+}) + S(\text{Mn}^{3+}) + S(\text{Mn}^{4+}) - S(\text{Fe}^{3+}) \\ &= 3,869 + 0,65 \times 2 + 0,33 \times 1,5 - 0,02 \times 2,5 = 5,614. \end{aligned}$$

- Gyromagnetic factor (g) determination:

$$g(\text{Nd}^{3+}) = 1 + \frac{J(J+1) + S \cos \theta (S \cos \theta + 1) - L(L+1)}{2J(J+1)} = 1 + \frac{5,754 \times 6,754 + 0,246 \times 1,246 - 6 \times 7}{2 \times 5,754 \times 6,754} = 0,96.$$

for all the sample $g = 0,67 \times 0,96 + 0,65 \times 2 + 0,33 \times 2 + 0,02 \times 2 = 2,6432$.

Figure 4 shows the evolution of M versus H at different T near T_C for the $\text{Nd}_{0,67}\text{Ba}_{0,33}\text{Mn}_{0,98}\text{Fe}_{0,02}\text{O}_3$ compound. The isothermal M (H, T) curves show a dependency between M and H at different T. Above T_C , a drastic decrease of $M(H, T)$ is observed with an almost linear behavior indicating a paramagnetic behavior. Below T_C , the curves show a nonlinear behavior with a sharp increase for

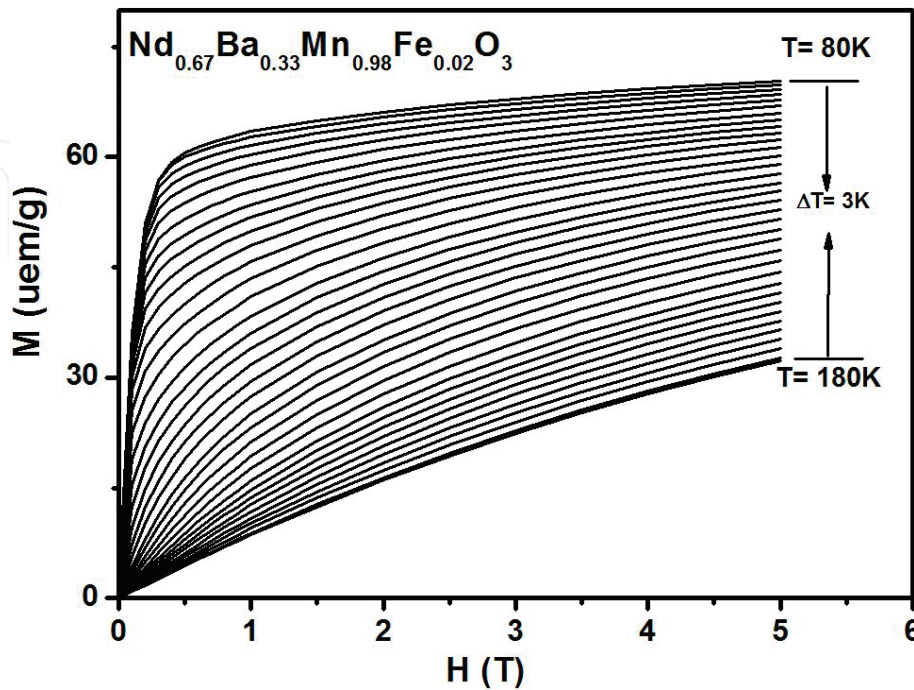


Figure 4. Isotherm magnetization M as a function of magnetic field H, measured for different temperatures with a step of 3 K for $\text{Nd}_{0,67}\text{Ba}_{0,33}\text{Mn}_{0,98}\text{Fe}_{0,02}\text{O}_3$ sample.

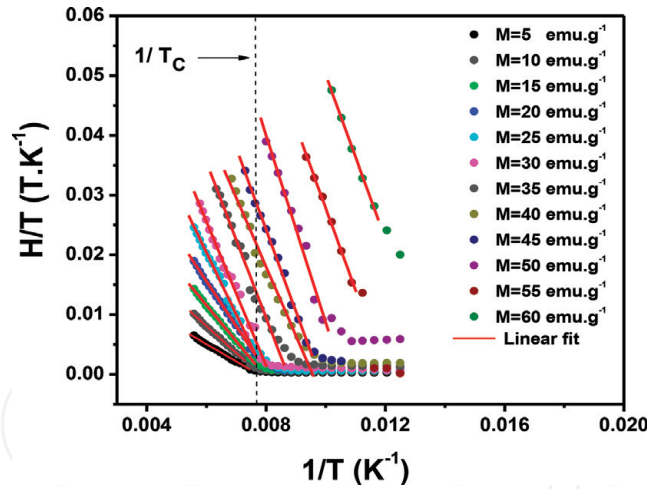


Figure 5. $\frac{H}{T}$ versus $\frac{1}{T}$ curves with constant values of magnetization per curve for $Nd_{0.67}Ba_{0.33}Mn_{0.98}Fe_{0.02}O_3$ sample.

low field values and a tendency to saturation, as field increases, reflecting a ferromagnetic behavior. Using **Figure 4**, we could plot the evolution of $\frac{H}{T}$ versus $\frac{1}{T}$ taken at constant values of magnetization M (5 emu.g^{-1} step) from 180 to 80 K in **Figure 5**. A linear behavior of the isomagnetic curves, which are progressively shifted into higher $\frac{1}{T}$ values, could be observed. So, the linear relationship between $\frac{H}{T}$ and $\frac{1}{T}$ is preserved. To find the value of the parameter λ , it is necessary to study H_{exch} induced by magnetization change. Linear fits are then kept at each isomagnetics line. Using Eq. (6), the slope of each isomagnetics line could give the suitable H_{exch} value. In **Figure 6**, we have plotted H_{exch} vs. M for the $Nd_{0.67}Ba_{0.33}Mn_{0.98}Fe_{0.02}O_3$ compound. For all materials, in the PM or antiferromagnetic domain, we can always expand increasing H in powers of M or M in powers of H . In this approach, we will stop at the third order, and considering that the M is an odd function of H [24, 31], we can write

$$H_{\text{exch}} = \lambda_1 M + \lambda_3 M^3 \quad (27)$$

Then, these points in **Figure 6** (H_{exch} versus M) should be included for the fit by Eq. (27).

However, a very small dependence on M^3 ($\lambda_3 = -0.00006 \text{ (T.emu}^{-1}.\text{g)}^3$) is noted for this second-order transition system. So, we can assume that $H_{\text{exch}} \approx \lambda M$,

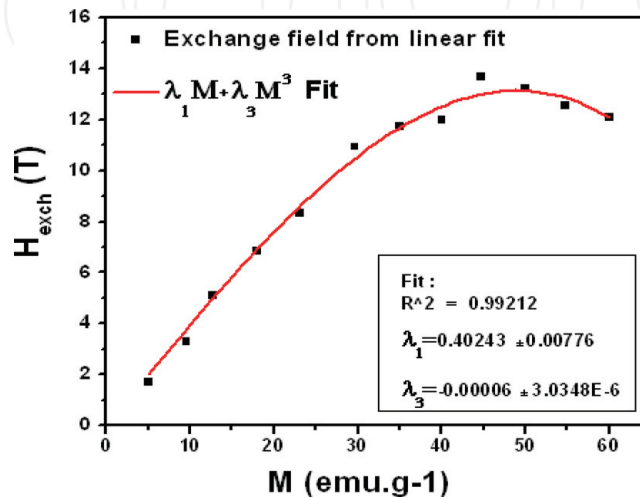


Figure 6. Exchange field versus magnetization for $Nd_{0.67}Ba_{0.33}Mn_{0.98}Fe_{0.02}O_3$ sample, with the function $\lambda_1 M + \lambda_3 M^3$ fit.

with $\lambda = \lambda_1 = 0.40243 \text{ T}\cdot\text{emu}^{-1}\cdot\text{g}$. Next, the building of the scaling plot M versus $\frac{H+H_{\text{exch}}}{T}$ is depicted in **Figure 7** with black symbols. It is clear from this figure that all these curves converge into one curve which can be adjusted by Eq. (6) using MATLAB software to determine M_0 , J , and g . We have found a good agreement between adjusted and theoretical parameters given in **Table 1**.

The agreement between fitted and theoretical values affirms the coupling between spins indicated above.

From the formula $\lambda = \frac{3k_B T_C}{NJ(J+1)g^2\mu_B^2}$ and $M_0 = NJg\mu_B$ and there adjusted values, we can estimate the value of the spin number N :

$$\left\{ \begin{array}{l} N = \frac{3k_B T_C}{\lambda J(J+1)g^2\mu_B^2} = \frac{3 \times 1,30807 \times 131.10^{-23}}{0,4024 \times 5,603 \times (5,603 + 1) \times 2,498^2 \times (9,274.10^{-24})^2} \approx 6.10^{23} \text{ (a)} \\ N = \frac{M_0}{Jg\mu_B} = \frac{83,592}{5.603 \times 2,6432 \times 9,274.10^{-24}} \approx 6.10^{23} \text{ (b)} \end{array} \right.$$

The two equalities, (a) and (b), practically give the same spin number N with verifying the validity of the mean field theory. In addition, the value of N is near to Avogadro number N_A . This implies that we can assume that molecule may be present in a same value of spin so an important order domain and the nonmagnetic molecules (impurities are very limited).

After injecting adjusted parameters λ , J , g , and M_0 in Eq. (6), we can get simulated M versus H curves (red lines), which are plotted with the experimental

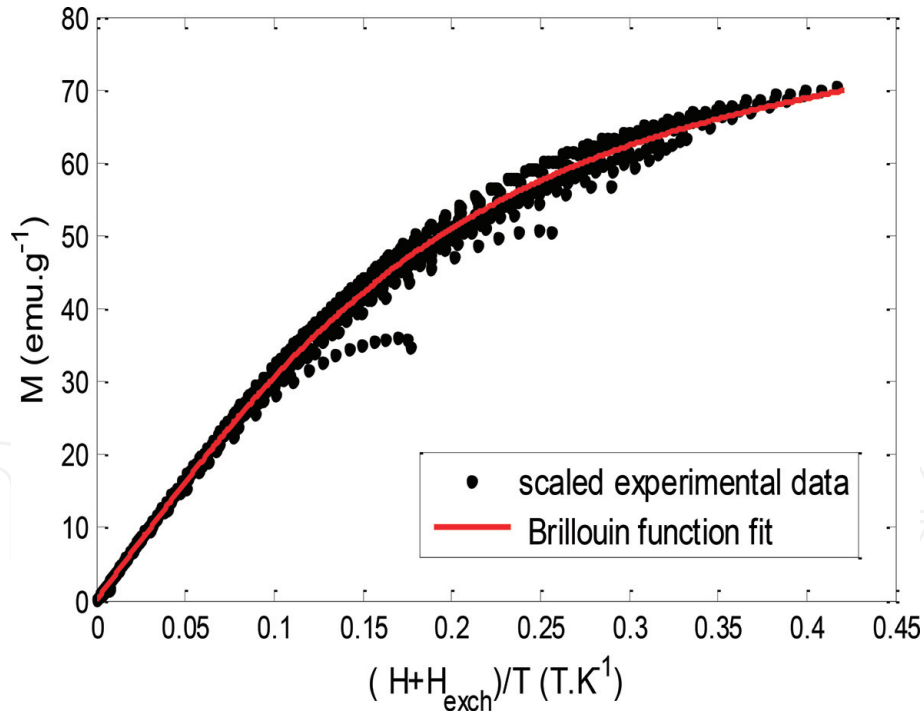


Figure 7.

Scaled data in magnetization versus $\frac{H+H_{\text{exch}}}{T}$ and Brillouin function fit for $\text{Nd}_{0.67}\text{Ba}_{0.33}\text{Mn}_{0.98}\text{Fe}_{0.02}\text{O}_3$ sample.

Parameters	J	g	M_0 ($\text{emu}\cdot\text{g}^{-1}$)
Theoretical values	5.614	2.643	—
Adjusted values	5.603	2.686	83.59

Table 1.

Theoretical and adjusted parameters of $\text{Nd}_{0.67}\text{Ba}_{0.33}\text{Mn}_{0.98}\text{Fe}_{0.02}\text{O}_3$ sample.

ones (black symbols) in **Figure 8**. This figure shows a good agreement between theoretical and experimental results. This illustrates the validity of the mean field to model the magnetization. On the other hand, **Figure 9** shows that simulated M versus T curves (red line) under various H are correlated with experimental ones

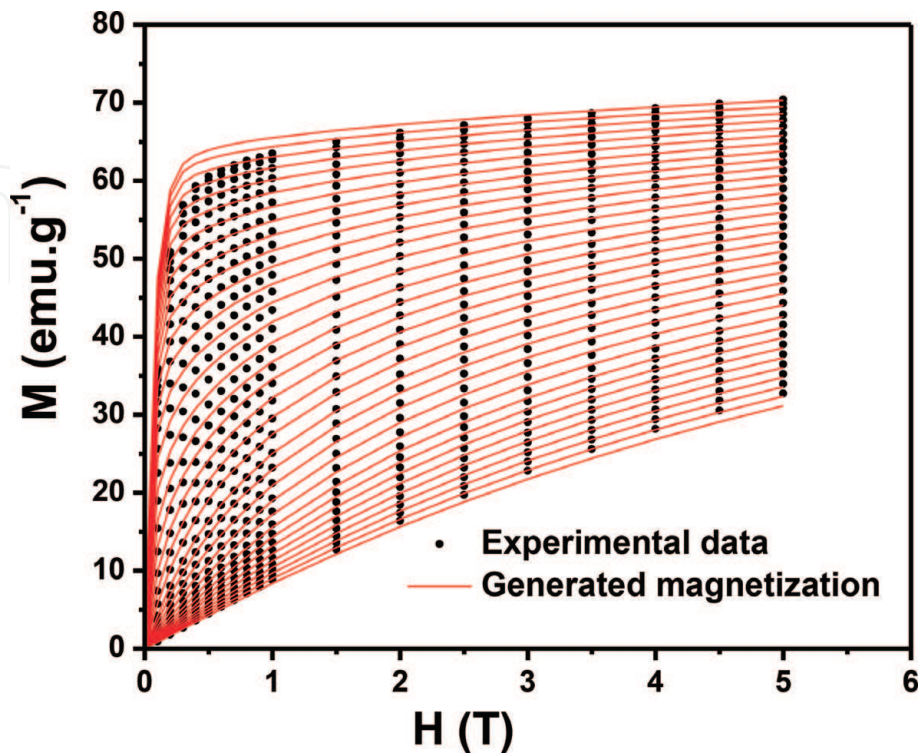


Figure 8.
Experimental M versus H (black symbols) of $Nd_{0.67}Ba_{0.33}Mn_{0.98}Fe_{0.02}O_3$ sample and the interpolation using the mean field method (red lines).

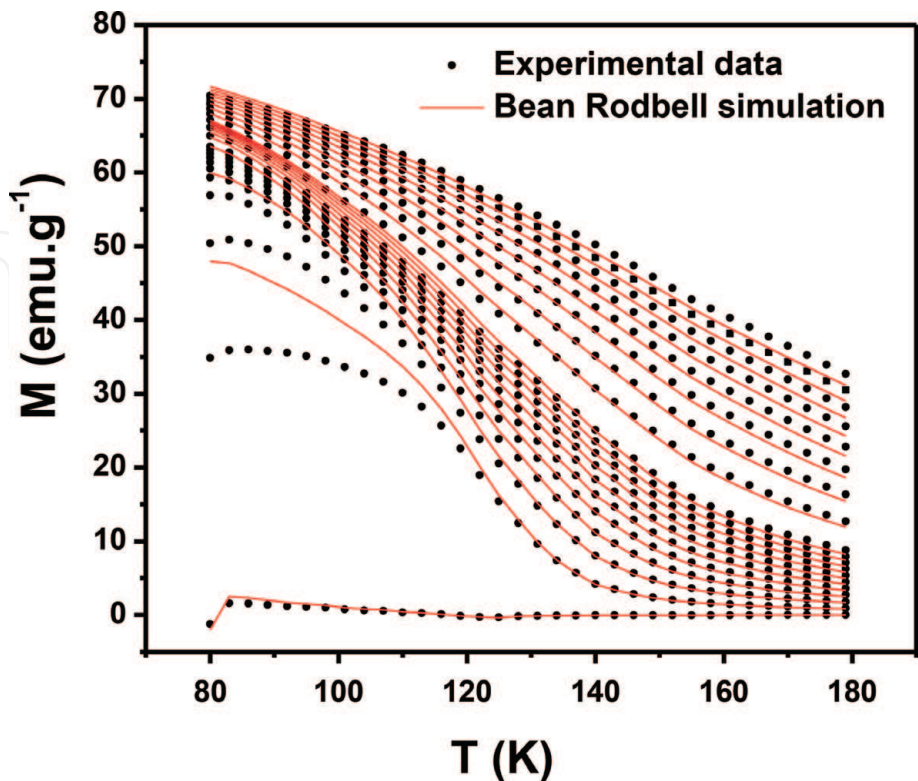


Figure 9.
Experimental magnetization versus T (black symbols) of $Nd_{0.67}Ba_{0.33}Mn_{0.98}Fe_{0.02}O_3$ sample and the interpolation using the Bean-Rodbell model (red lines).

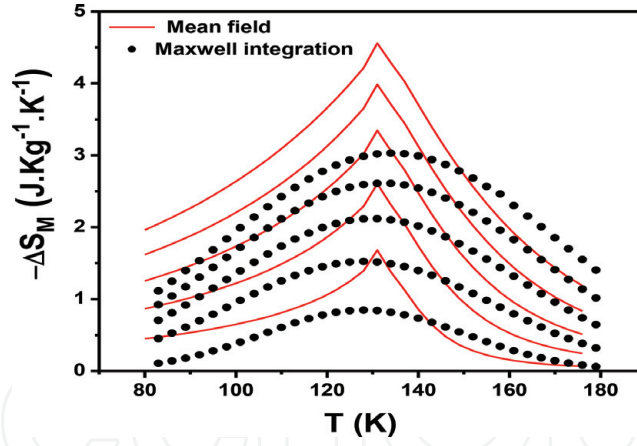


Figure 10.

Experimental and theoretical magnetic entropy change $-\Delta S_M$ versus T of $Nd_{0.67}Ba_{0.33}Mn_{0.98}Fe_{0.02}O_3$ sample as a function of temperature upon different magnetic field intervals (ΔH).

Method	H (T)	1	2	3	4	5
Maxwell relation	δT_{FWHM} (k)	47.54	54.34	56.98	59.15	63.01
	$-\Delta S_M^{max}$ (J.Kg $^{-1}$.K $^{-1}$)	0.85	1.53	2.12	2.62	3.04
	RCP(J.Kg $^{-1}$)	40.41	83.14	120.80	154.97	191.55
Mean field theory	δT_{FWHM} (k)	27.28	33.31	39.83	41.51	44.18
	$-\Delta S_M^{max}$ (J.Kg $^{-1}$.K $^{-1}$)	1.65	2.59	3.32	3.98	4.54
	RCP(J.Kg $^{-1}$)	45.01	86.27	132.24	165.2	200.58

Table 2.

Comparative between δT_{FWHM} , $-\Delta S_M^{max}$, and RCP calculated graphically using Maxwell relation and mean field theory.

(black symbols) when $\eta = 0.32$ and $T_0 = 131$ K. Thus, the second-order phase transition of this compound is reconfirmed with the η parameter value ($\eta < 1$).

Figure 10 shows simulated $-\Delta S_M$ versus T curves (red lines) using Eq. (9b) and the experimental ones (black symbols) using the Maxwell relation from in Eq. (9a). As seen in this figure and taking account into the initial considering of H and M as an internal and external variable in Eq. (8a) and vice versa in Eq. (8b), $-\Delta S_M$ estimated in these two considerations is little different. This aspect has been reported in the work of Amaral et al. [18]. From **Figure 10**, we can estimate the full width at half maximum δT_{FWHM} , the maximum magnetic entropy change $-\Delta S_M^{max}$, and the relative cooling power (RCP) which is the product of $-\Delta S_M^{max}$ and δT_{FWHM} . These magnetocaloric properties are listed in **Table 2**.

As shown in **Table 2**, a rising of $-\Delta S_M^{max}$ obtained by using the mean field model could be noted. For example, it exceeds the one determined by using the classical Maxwell relation by $1.5 \text{ J.Kg}^{-1}.\text{K}^{-1}$ under 5 T applied field. Although δT_{FWHM} determined by this method seems less, RCP values are more higher than those obtained from the Maxwell relation. As a result, the mean field model could amplify RCP. This novel method has so better performance than the classical Maxwell relation.

Considering the number of magnetic near neighbors ions, z , in our material and its critical temperature, the relation $J = \frac{3k_B T_c}{2zJ+1}$ (Eq. (26)) allows us to find the Heisenberg exchange constant J . In the perovskite structure of $Nd_{0.67}Ba_{0.33}Mn_{0.98}Fe_{0.02}O_3$ compound, the Mn ion placed at the center of the pseudo-cubic cell has four near neighbors Nd distant from $\frac{a\sqrt{3}}{2}$ and six near

neighbors Mn distant from a and similarly for Nd. The interaction is established between Mn-Mn and Mn-Nd or Nd-Nd and Nd-Mn.

By averaging these interactions, the relationship (19) should be written as

$$J = \frac{3k_B T_c}{2} \times \frac{1}{\left[\frac{z_{Mn}S(S+1) + z_{Mn-Nd}J_{Mn-Nd}(J_{Mn-Nd}+1) + z_{Nd}J(J+1)}{3} \right]}$$

where $z_{Mn-Mn} = 6$, $z_{Mn-Nd} = 4$, and $z_{Nd-Nd} = 6$

$$\begin{aligned} S(\text{Mn, Fe}) &= S(\text{Mn}^{3+}) + S(\text{Mn}^{4+}) - S(\text{Fe}^{3+}) \\ &= 0.65 \times 2 + 0.33 \times 1,5 - 0,02 \times 2,5 = 1.3 + 0.495 - 0.05 = 1.745; \end{aligned}$$

$J_{Nd} = 3.855$; $J_{Mn-Nd} = 5.66$. So, $J = \frac{3 \times 1.3807 \times 10^{-23} \times 131}{2} \times \left[\frac{1}{\frac{6 \times 1.745 \times 2.745 + 4 \times 5.6 \times 6.6 + 6 \times 3.855 \times 4.855}{3}} \right]$
 $= 2.8175 \times 10^{-23}$ joules for magnetic ion in our sample. This value explains the strength interaction between spins. Moreover, it is a crucial parameter used in the simulation with the Monte Carlo method.

3. Conclusion

In this work, we have analyzed the mean field scaling method for the Nd_{0.67}Ba_{0.33}Mn_{0.98}Fe_{0.02}O₃ sample. The perspicacity saved from the usefulness of this method for a magnetic system could be of large interest. In a simple reason, we can consider that if this scaling method does not follow the mean field behavior, other methods need to be convinced in the interpretation of the system's magnetic behavior. The mean field scaling method allows us to estimate the exchange parameter λ , the total angular momentum (J), the gyromagnetic factor g, the number of spins N of our sample, the saturation magnetization M_0 , and the Heisenberg exchange constant J. Some of these factors are useful in estimating some magnetic properties. The mean field and the Bean-Rodbell models allow to follow the evolution of generated magnetization curves as function as the applied field and the temperature. A good agreement between theoretical and experimental magnetizations has been noted. The dependence of the entropy change on temperature under various applied fields has been experimentally and theoretically derived. An acceptable agreement between theoretical and experimental results is observed. However, the performance of RCP has been granted by the mean field model. Also, intervention of the Bean-Rodbell model confirms the second-order magnetic transition of our sample. Because this type of transition is needed for evaluating the MCE, a significant theoretical description of magnetic and magnetocaloric properties of the Nd_{0.67}Ba_{0.33}Mn_{0.98}Fe_{0.02}O₃ sample should be taking into account and should be accordable with other models.

IntechOpen

IntechOpen

Author details

Mohamed Hsini* and Sadok Zemni
Faculty of Science Monastir, Sidi Bouzid, Tunisia

*Address all correspondence to: mohamed.hsini.14@gmail.com

IntechOpen

© 2019 The Author(s). Licensee IntechOpen. This chapter is distributed under the terms of the Creative Commons Attribution License (<http://creativecommons.org/licenses/by/3.0>), which permits unrestricted use, distribution, and reproduction in any medium, provided the original work is properly cited. 

References

- [1] Phan MH, Yu SC. Review of the magnetocaloric effect in manganite materials. *Journal of Magnetism and Magnetic Materials*. 2007;**308**:325-340. DOI: [org/10.1016/j.jmmm.2006.07.025](http://dx.doi.org/10.1016/j.jmmm.2006.07.025)
- [2] Kitanovski A, Egolf PW. Application of magnetic refrigeration and its assessment. *Journal of Magnetism and Magnetic Materials*. 2009;**321**:777-781. DOI: [10.1016/j.jmmm.2008.11.078](http://dx.doi.org/10.1016/j.jmmm.2008.11.078)
- [3] Ke YJ, Zhang XQ, Ma Y, Cheng ZH. Anisotropic magnetic entropy change in $RFeO_3$ single crystals ($R = Tb, Tm, \text{ or } Y$). *Chinese Physics B*. 2015;**24**:037501. DOI: [10.1038/srep19775](http://dx.doi.org/10.1038/srep19775)
- [4] Wada H, Tanabe Y. Giant magnetocaloric effect of $MnAs_{1-x}Sb_x$. *Applied Physics Letters*. 2001;**79**:3302. DOI: [10.1063/1.1419048](http://dx.doi.org/10.1063/1.1419048)
- [5] Balli M, Fruchart D, Gignoux D. A study of magnetism and magnetocaloric effect in $Ho_{1-x}Tb_xCo_2$ compounds. *Journal of Magnetism and Magnetic Materials*. 2007;**314**:16-20. DOI: [10.1016/j.jmmm.2007.02.007](http://dx.doi.org/10.1016/j.jmmm.2007.02.007)
- [6] Tishin AM, Spichkin YI. *The Magnetocaloric Effect and Its Applications*. London: IOP Publishing; 2003
- [7] Dong Q, Zhang H, Sun J, Shen B, Franco V. Magnetocaloric response of $Fe_{75}Nb_{10}B_{15}$ powders partially amorphized by ball milling. *Journal of Applied Physics*. 2008;**103**:116101. DOI: [10.1063/1.3155982](http://dx.doi.org/10.1063/1.3155982)
- [8] De Oliveira N. Magnetocaloric effect in the pseudobinaries $(Ho_{1-c}Rc)Co_2$ ($R = Er \text{ and } Dy$). *Eur. Phys. J. B*. 2008;**65**:207-212. DOI: [10.1140/epjb/-2008-00346-y](http://dx.doi.org/10.1140/epjb/-2008-00346-y)
- [9] Wang ZW, Yu P, Cui YT, Xia L. Near room temperature magneto-caloric effect of a $Gd_{48}Co_{52}$ amorphous alloy. *Journal of Alloys and Compounds*. 2016; **658**:598-602. DOI: [10.1016/j.jallcom.2015.10.293](http://dx.doi.org/10.1016/j.jallcom.2015.10.293)
- [10] Hamad MA. Magnetocaloric effect in $La_{0.7}Sr_{0.3}MnO_3/Ta_2O_5$ composites. *J. A. D.* 2013;**2**:213-217. DOI: [10.1007/s40145-013-0062-0](http://dx.doi.org/10.1007/s40145-013-0062-0)
- [11] Phejar M, Paul-Boncour V, Bessais L. Investigation on structural and magnetocaloric properties of $LaFe_{13-x}Si_x(H,C)_y$ compounds. *Journal of Solid State Chemistry*. 2016;**233**:95-102. DOI: [org/10.1016/j.jssc.2015.10.016](http://dx.doi.org/10.1016/j.jssc.2015.10.016)
- [12] Tlili R, Omri A, Bejar M, Dhahri E, Hlil EK. Theoretical investigation of the magnetocaloric effect of $La_{0.7}(Ba, Sr)_{0.3}MnO_3$ compound at room temperature with a second-order magnetic phase transition. *Ceramics International*. 2015; **41**:10654-10658. DOI: [10.1016/j.ceramint.2015.04.165](http://dx.doi.org/10.1016/j.ceramint.2015.04.165)
- [13] Tlili R, Hammouda R, Bejar M, Dhahri E. Effect of Ga substitution on magnetocaloric effect in $La_{0.7}(Ba, Sr)_{0.3}Mn_{1-x}Ga_xO_3$ ($0.0 \leq x \leq 0.20$) polycrystalline at room temperature. *Journal of Magnetism and Magnetic Materials*. 2015;**399**:143-148. DOI: [10.1016/j.jmmm.2015.09.073](http://dx.doi.org/10.1016/j.jmmm.2015.09.073)
- [14] Raju K, Pavan Kumar N, Venugopal Reddy P, Yoon DH. Influence of Eu doping on magnetocaloric behavior of $La_{0.67}Sr_{0.33}MnO_3$. *Physics Letters A*. 2015;**379**:1178-1182. DOI: [10.1016/j.physleta.2015.02.016](http://dx.doi.org/10.1016/j.physleta.2015.02.016)
- [15] Coey J. *Magnetism and Magnetic Materials*. Cambridge: Cambridge University Press; 2009
- [16] Kittel C. *Introduction to Solid State Physics*. 7th ed. New York: Wiley; 1996
- [17] Gonzalo JA. *Effective Field Approach to Phase Transitions and Some Applications to Ferroelectrics*. Singapore: World Scientific; 2006

- [18] Amaral JS, Das S, Amaral VS. The meanfield theory in the study of ferromagnets and the magnetocaloric effect, thermodynamics —systems in equilibrium and nonequilibrium. In: Piraj'a JCM, editor. Rijeka, Croatia: InTech; 2011. Available from: <https://www.intechopen.com/books/thermodynamics-systems-in-equilibrium-and-non-equilibrium/th0.33emean-field-theory-in-the-study-of-ferromagnets-and-the-magnetocaloric-effect>
- [19] Hcini S, Boudard M, Zemni S, Oumezzine M. Effect of Fe-doping on structural, magnetic and magnetocaloric properties of $\text{Nd}_{0.67}\text{BaMn}_{1-x}\text{Fe}_x\text{O}_3$ manganites. *Ceramics International*. 2014;**40**:16041-16050. DOI: 10.1016/j.ceramint.2014.07.140
- [20] Dong QY, Zhang HW, Sun JR, Shen BG, Franco V. A phenomenological fitting curve for the magnetocaloric effect of materials with a second-order phase transition. *Journal of Applied Physics*. 2008;**103**:116101-1161015. DOI: 10.1063/1.2913166
- [21] Bean CP, Rodbell DS. Magnetic disorder as a first-order phase transformation. *Physics Review*. 1962; **126**:104-115. DOI: 10.1103/PhysRev.126.104
- [22] Baazaoui M, Boudard M, Zemni S. Magnetocaloric properties in $\text{Ln}_{0.67}\text{Ba}_{0.33}\text{Mn}_{1-x}\text{Fe}_x\text{O}_3$ (Ln=La or Pr) manganites. *Materials Letters*. 2011;**65**: 2093-2095. DOI: 10.1016/j.matlet.2011.04.051
- [23] Mostafa AG, Abdel-Khalek EK, Daoush WM, Moustafa SF. Study of some co-precipitated manganite perovskite samples-doped iron. *Journal of Magnetism and Magnetic Materials*. 2008;**320**:3356-3360. DOI: 10.1016/j.jmmm.2008.07.025
- [24] Ogale SB, Shreekala R, Bathe R, Date SK, Patil SI, Hanoyer B, et al. Transport properties, magnetic ordering, and hyperfine interactions in Fe-doped $\text{La}_{0.75}\text{Ca}_{0.25}\text{MnO}_3$: Localization-delocalization transition. *Physical Review B*. 1998;**57**:7841. DOI: 10.1103/PhysRevB.57.7841
- [25] Callen HB. *Thermodynamics and an Introduction to Thermostatistics*. 2nd ed. New York: Wiley; 1985
- [26] Von Ranke PJ, de Oliveira NA, Gama S. Understanding the influence of the first-order magnetic phase transition on the magnetocaloric effect: Application to $\text{Gd}_5(\text{Si}_x\text{Ge}_{1-x})_4$. *Journal of Magnetism and Magnetic Materials*. 2004;**2(77)**:78-83. DOI: 10.1016/j.jmmm.2003.10.013
- [27] Turcaud JA, Pereira AM, Sandeman KG, Amaral JS, Morrison K, Berenov A, et al. Spontaneous magnetization above T_C in polycrystalline $\text{La}_{0.7}\text{Ca}_{0.3}\text{MnO}_3$ and $\text{La}_{0.7}\text{Ba}_{0.3}\text{MnO}_3$. *Physical Review B*. 2014;**90**:024410-024417. DOI: 10.1103/PhysRevB.90.024410
- [28] Balli M, Fruchart D, Gignoux D, Tobola J, Hlil EK, Wolfers P, et al. Magnetocaloric effect in ternary metal phosphides $(\text{Fe}_{1-x}\text{Ni}_x)_2\text{P}$. *Journal of Magnetism and Magnetic Materials*. 2007;**316**:358-560. DOI: 10.1016/j.jmmm.2007.03.018
- [29] Zach R, Guillot M, Tobola J. Semiquantitative analysis of magnetic phase transitions in the $\text{MnFeP}_{1-x}\text{As}_x$ series of compounds. *Journal of Applied Physics*. 1998;**83**:7237-7239. DOI: 10.1063/1.367856
- [30] Jia L, Sun J, Zhang H, Hu F, Dong C, Shen B. Magnetovolume effect in intermetallics $\text{LaFe}_{13-x}\text{Si}_x$. *Journal of Physics: Condensed Matter*. 2006;**18**: 9999-10009. DOI: 10.1088/0953-8984/18/44/002
- [31] Cyrot M. *Magnetisme I—Fondements*. Grenoble: Presses Universitaires de Grenoble; 1999